

Multicomponent Sorption of Hexane Isomers in Zeolite BETA

Patrick S. Bárcia and José A. C. Silva

Escola Superior de Tecnologia e Gestão, Instituto Politécnico de Bragança, Apartado 1134, 5301-857 Bragança, Portugal

Alírio E. Rodrigues

Faculdade de Engenharia, Departamento de Engenharia Química, Laboratory of Separation and Reaction Engineering, Universidade do Porto, Rua do Dr. Roberto Frias, S/N, 4200-465 Porto, Portugal

DOI 10.1002/aic.11233

Published online June 15, 2007 in Wiley InterScience (www.interscience.wiley.com).

Breakthrough curves of single, binary, ternary, and quaternary mixtures of hexane (C₆) isomers n-hexane (nHEX), 3-methylpentane (3MP), 2,3-dimethylbutane (23DMB), and 2,2-dimethylbutane (22DMB) were performed in commercial pellets of zeolite BETA (BEA structure), covering the temperature range between 423 and 523 K and partial pressures up to 30 kPa. From these data, single and multicomponent adsorption equilibrium isotherms were collected. A tri-site Langmuir model (TSL) was developed to interpret the equilibrium data based on considerations about zeolite structure, and a dynamic adsorption model was tested predicting with a good accuracy the behavior of multicomponent fixed-bed experiments. At the partial pressures studied, the sorption hierarchy in the zeolite BETA is nHEX >>> 3MP > 23DMB >> 22DMB. BEA structure demonstrates a significant selectivity between C₆ isomers, especially at low coverage, giving a good perspective regarding their separation by adsorption processes. © 2007 American Institute of Chemical Engineers AIChE J, 53: 1970–1981, 2007
Keywords: zeolite BETA, hexane isomers separation, multicomponent adsorption, breakthrough curves, dynamic adsorption model

Introduction

Along the last decades, the refining industry has attempted to enhance the octane quality of the gasoline fulfilling the environmental standards imposed. This continuous effort began in 1970, when Shell started the first hydroisomerization reactor, the *Hysomer*, whose function is to convert the low RON linear paraffins into high RON branched ones by catalytic reaction at a temperature range between 500 and 550 K. However, this reaction is incomplete and a large fraction of linear molecules remain in the output isomerate. To overcome this problem, Universal Oil Products (UOP) coupled to this reactor an adsorption unit, named *IsoSiv*, packed with zeolite 5A. This unit removes the normal paraf-

fins from the output of the catalytic reactor, and recycles this stream for complete conversion in the *Hysomer*. The resulting cluster is known as the Total Isomerization Process (TIP) and the octane enhancement results in an isomerate having an octane of about 90 RON. However, the data from UOP reveal that 30% of the typical composition of the isomerate from the actual TIP consists of low RON monobranched C₆ isomers.¹

Nowadays, the phase-out of the MTBE in several parts of the United States stresses the need for alternative solutions that can improve the quality of the gasoline without additives. Our idea consists in optimizing the actual TIP incorporating a second adsorption unit packed with a proper adsorbent, with the goal of removing the low RON monobranched C₆ isomers from the output of the TIP, and recycling it to the catalytic reactor. With this extra unit, and considering the data from UOP, it is possible to obtain a highest octane isomerate having about 96 RON.

Correspondence concerning this article should be addressed to A. E. Rodrigues at arodrig@fe.up.pt.

The study of the separation of monobranched and dibranched C_6 isomers mixtures is essential for octane number enhancement in a cyclic adsorption process. From an engineering point of view, it is of great importance that selectivity is high at low coverage, since if that occurs the additional costs in the desorption stage (clean-up of the bed) are minimized. Cleaning-up a strongly saturated adsorbent in a fixed bed is energetically more demanding and consequently more expensive. For instance, in a Configurational-Bias Monte Carlo (CBMC) simulation study, Schenk et al.² found that the sorption selectivity of an equimolar mixture of 22DMB/3MP in MFI zeolite structure at 362 K only increases significantly for a coverage greater than 4 molecules per unit cell (corresponding approximately to 6 g/100 g_{ads}), which seems to be a very high charge. In an experimental study, Jolimaire et al.³ show that the separation between 22DMB and 2MP is possible in silicalite, being the separation based in kinetic considerations regarding the slow diffusion of 22DMB in the zeolite structure. In this study, the capability is checked of zeolite BETA to separate low RON monobranched C_6 isomers from a mixture containing high RON dibranched C_6 isomers. Furthermore, we intend to carry out this separation at low coverage (lower than 6 g/100 g_{ads}) and in a temperature range similar to the operational conditions of the TIP.

Zeolite BETA is a large pore size adsorbent of great importance in catalytic processes of the refining industry; however, its functionality as adsorbent in separation processes is scarcely explored.⁴ It is reported that in zeolite BETA structure, there are two types of mutually intersecting channels with different pore aperture dimensions similar to the kinetic diameter of the C_6 isomers. This characteristic can be advantageous to carry out the separation exploiting the conformation of the molecules. Some studies of equilibrium of adsorption on zeolite BETA suggest a relatively good selectivity for separating C_6 isomers. Huddersman and Klimczyk⁵ indicates that zeolite BETA in cation form (H,Ba) is an effective separating media for branched C_6 isomers, superior to silicalite. Moreover, in previous studies of sorption of C_6 isomers in zeolite BETA, Bárcia et al.^{6,7} noticed that in the low partial pressure range (or low loading), the amount adsorbed of n HEX and 3MP is higher than that of 22DMB and 23DMB; besides, it was demonstrated that zeolite BETA exhibits a significant degree of selectivity for a binary equimolar mixture of 22DMB/3MP giving a good perspective regarding the development of a cyclic separation process, for the separation of mono and dibranched isomers.

The goal of this work is to study the simultaneous sorption of C_6 isomers. We start by giving an overview of the experimental procedure, and we present an expanded tri-site Langmuir model (TSL) for the interpretation of the sorption of C_6 isomers in BEA structure. The pure component experimental data are fitted with this model; and then the model is extended to predict the binary, ternary, and quaternary mixture sorption data and results compared with the experimental ones. On the basis of the sorption equilibrium and selectivity data, we have discussed the sorption events at molecular level. Multicomponent breakthrough experiments are presented and a dynamic mathematical model is used to simulate the fixed-bed experiments using the experimental equilibrium sorption data. Tips regarding the best operating con-

ditions for separating hexane isomers in zeolite BETA are addressed.

Experimental

Characterization of the adsorbent and C_6 isomers

The pellets used in this work were 1/16 in. cylindrical extrudates of zeolite BETA (Si/Al = 150), provided by SUD-CHEMIE AG with an average length of 5 mm. In Table 1, mercury porosimetry results of the pellets performed by LABGRAN at the University of Coimbra (Portugal) are reported.

Figure 1 shows that the zeolite BETA structure consists of a three-dimensional channel system composed by straight and zigzag channels with the same 12-membered rings aperture, 0.66×0.67 nm. However, because of the arrangement of the zigzag channel, the resulting free aperture of this type of channels is 0.56×0.56 nm. It is also clear from the figure that both types of channels are mutually intersecting, creating an open space that can be favorable to the adsorption of the bulkier molecules.

An approximate three-dimensional structure of C_6 isomers is also shown in Figure 1. It can be seen that the structure of n HEX is linear, 3MP has one methyl branch, 23DMB and 22DMB two methyl branches with 22DMB having the substitution of the hydrogen by the methyl groups in the same carbon atom. The kinetic diameter of the molecules is also indicated, since it plays an important role in the sorption events conditioning the access of the bulkier molecules to the zig-zag channels of the zeolite BETA. According to the values of the kinetic diameters of the C_6 isomers and the channels aperture of zeolite BETA, the bulkier 22DMB and 23DMB can only access in principle the straight channels, while 3MP and n HEX can access both type of channels. Moreover, it is also possible to see from Figure 1 that the increase of the branching degree implies also the decrease of the length of the molecules.

All hydrocarbons used in this work were of analytical grade supplied by Sigma-Aldrich.

Table 1. Physical Properties of Zeolite BETA Crystals and Mercury Porosimetry Data of Pellets

Physical properties of crystals	
Structure type	H-BEA 150
Si/Al ratio, mol/mol	150
Particle dimensions, μm^a	0.25–0.40
Oxygen's in window	12
Crystal type	Tetragonal
Channel size, nm	$\langle 100 \rangle 0.66 \times 0.67^{(**)b} \leftrightarrow^c$ $[100] 0.56 \times 0.56^{(*)}$
Mercury porosimetry data of pellets	
S_{BET} , m^2/g	447.8
Intrusion volume, cm^3/g ($\approx 2\text{--}30,000$ psia) ^d	0.14
Apparent density, ρ_a (g/cm^3)	1.18
Solid density, ρ_s (g/cm^3) (30,000 psia)	1.42
Porosity, ϵ_p	0.17

^aDetermined by SEM.

^bThe number of asterisk indicated whether the channel system is one- or two-dimensional.

^cInterconnecting channel systems are separated by a double arrow (\leftrightarrow).

^dThe mercury porosimetry was performed by LABGRAN with a Poresizer 9320 of Micromeritics, which operate at pressures among 0.5 and 30,000 psia.

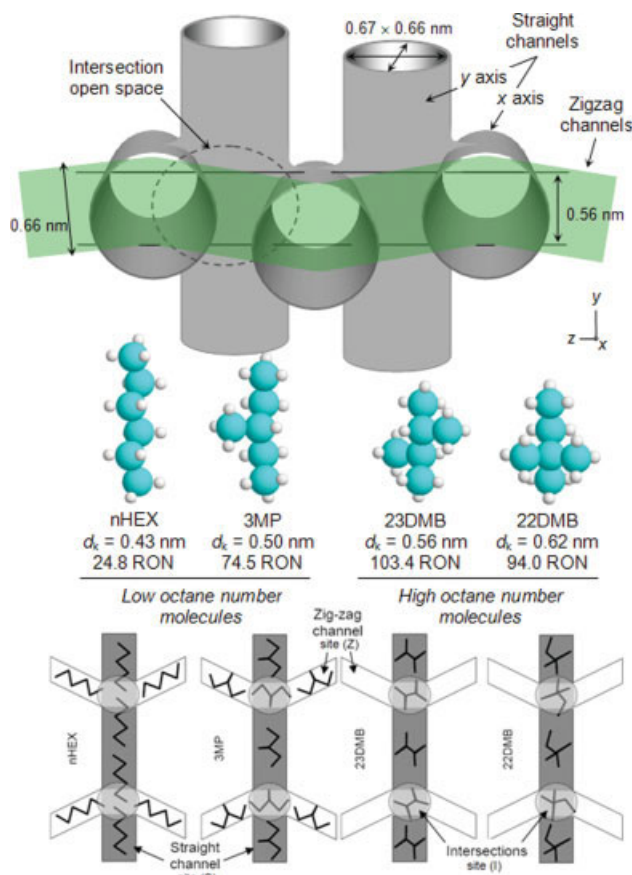


Figure 1. 3-D view of zeolite BETA framework and C₆ isomers with their kinetic diameter and octane number.

It is also shown a schematic representation of the sorption sites and the hypothetical location of hexane isomers in the zeolite BETA structure. [Color figure can be viewed in the online issue, which is available at www.interscience.wiley.com.]

Experimental setup

The experimental data was obtained in an apparatus developed for the measurement of single and multicomponent breakthrough curves consisting of three main sections. The preparation section includes a syringe pump used to introduce the adsorbable species in the carrier gas followed by a heating chamber where this stream is completely vaporized. The adsorption section consists of a 4.6 mm i.d. stainless steel column with 100 mm in length entirely filled with zeolite BETA pellets placed in a ventilated chromatographic oven, as well as a heated collector with 10 loops to collect samples at the outlet of the column. The third part is an analytical section composed by a chromatographic column and a flame ionization detector (FID). Complete information about the experimental setup is reported elsewhere.^{6,7}

Experimental procedure

Single and multicomponent adsorption equilibrium isotherms were obtained from breakthrough experiments. The adsorption column packed with pellets of zeolite BETA was operated by introducing continuously a C₆ isomers mixture with known composition in a helium stream at a fixed total

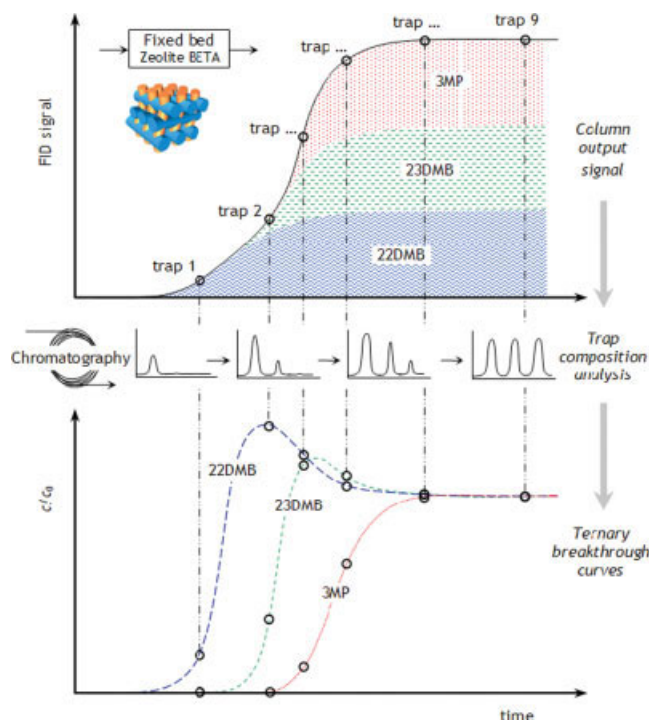


Figure 2. Experimental procedure used for the determination of the multicomponent sorption equilibrium (e.g., ternary mixture experiment).

[Color figure can be viewed in the online issue, which is available at www.interscience.wiley.com.]

pressure. Figure 2 shows a schematic representation of the procedure used to measure multicomponent breakthrough curves. It consists in measuring continuously the concentration profile at the outlet of the packed bed to collect samples during the most important part of the breakthrough curve. When the saturation is reached, the composition of each sample loop is evaluated by chromatography in a proper separate column.

Modeling adsorption equilibrium

Pure Component Isotherms. For the development of an adsorption process, it is important to obtain a good analytical

Table 2. Dynamic Mathematical Model Equations for Fixed-Bed Adsorption

Fixed-Bed Adsorption	Equations
Mass balance to sorbate species	$\varepsilon_b D_L \frac{\partial^2 c_i}{\partial z^2} = \frac{\partial(u c_i)}{\partial z} + \varepsilon_b \frac{\partial c_i}{\partial t} + (1 - \varepsilon_b) \rho_a \frac{\partial \bar{q}_i}{\partial t}$ (7)
Overall mass balance	$C \frac{\partial u}{\partial z} + \varepsilon_b \frac{\partial C}{\partial t} + \sum_{i=1}^N (1 - \varepsilon_b) \rho_a \frac{\partial \bar{q}_i}{\partial t} = 0$ (8)
Mass transfer rate	$\rho_a \frac{\partial \bar{q}_i}{\partial t} = k(q_i - \bar{q}_i)$ (9)
Axial dispersion ¹³ (Langer et al., 1978)	$\frac{1}{Pe} = \frac{D_L}{uL} = \gamma \frac{D_m}{uL} + \frac{d_p}{LP'_{\infty} \left(1 + \beta \frac{D_m}{uL}\right)}$ being, (10) $\gamma = 0.45 + 0.55 \varepsilon_b$, $Pe'_{\infty} = 670 \cdot d_p$ and $\beta = 10$

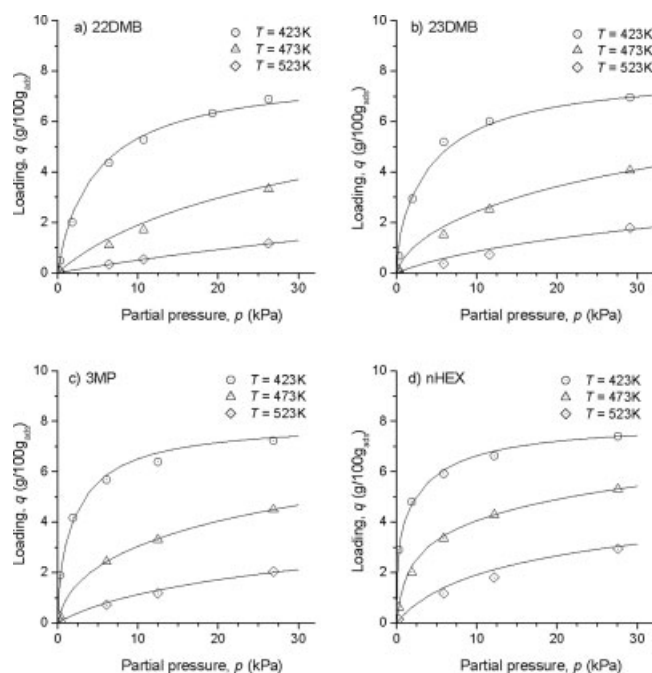


Figure 3. Pure component adsorption equilibrium isotherm of (a) 22DMB, (b) 23DMB, (c) 3MP, and (d) nHEX on pellets of zeolite BETA at 423, 473, and 523 K.

The continuous lines represent the fitting with the TSL model. The experimental conditions for the breakthrough experiments are specified in previous articles.^{6,7}

description of the experimental sorption data. For instance, Krishna et al.^{8,9} used the dual-site Langmuir (DSL) model isotherm to describe the pure component isotherms of several alkanes in zeolite MFI. The DSL model distinguishes two categories of sorption sites in the adsorbent (one at the channels and the other at the intersections) each one following a

Langmuir adsorption behavior. The adsorption isotherm is

$$q(p, T) = q_m^S \frac{b^S(T)p}{1 + b^S(T)p} + q_m^Z \frac{b^Z(T)p}{1 + b^Z(T)p} \quad (1)$$

where q is the amount adsorbed, p is the pressure of sorbate, b and q_m are the adsorption affinity constant and the saturation loading in each type of sites, respectively. Here, the superscripts S and Z indicate whether the sites are in straight or zig-zag channel, respectively.

For zeolite BETA, this isotherm seems equally interesting since there are two different types of channels that can give different kinds of active sites for sorption.^{6,7} However, an extended multicomponent DSL model does not fit well the ternary and quaternary multicomponent data shown through this work. Also, the ideal adsorbed solution (IAS) theory with the DSL model was used to predict, but without success, the multicomponent sorption equilibrium data. To correlate all the experimental data of sorption equilibrium of the C_6 isomers on zeolite BETA, it was assumed that the open space at the channels intersection of zeolite BETA can also represent a different category of active sites (see Figure 1). Thus, the Langmuir model is expanded to describe the sorption behavior in three different categories of active sites resulting in a TSL model isotherm, i.e., a linear superposition of three Langmuir isotherms reflecting the heterogeneity of the adsorbent. The resulting isotherm is

$$q(p, T) = q_m^S \frac{b^S(T)p}{1 + b^S(T)p} + q_m^Z \frac{b^Z(T)p}{1 + b^Z(T)p} + q_m^I \frac{b^I(T)p}{1 + b^I(T)p} \quad (2)$$

Here, the superscripts S , Z , and I indicate whether the adsorption sites are in a straight or zig-zag channel or in an intersection, respectively. It is shown at the bottom of Figure 1, a simplified schematic representation of the hypothetical localization of different types of sorption sites and the preferential location of each C_6 isomers molecules in the

Table 3. TSL Model Parameters and Deviations Between Model and Experiments

Parameter	Unit	22DMB	23DMB	3MP	nHEX
q_m^I	(g/100 g _{ads})	1.15	1.33	3.49	0.96
b_0^I	(kPa ⁻¹)	3.21×10^0	6.83×10^{-1}	4.98×10^{-3}	4.63×10^{-3}
b^I (423 K)	(kPa ⁻¹)	0.8330	5.4494	0.2873	9.8761
b^I (473 K)	(kPa ⁻¹)	0.1075	0.4894	0.0209	0.4913
b^I (523 K)	(kPa ⁻¹)	0.0205	0.0697	0.0025	0.0434
$-\Delta H^I$	(kJ/mol)	68.13	80.18	87.14	99.84
q_m^S	(g/100 g _{ads})	6.85	6.67	2.83	4.55
b_0^S	(kPa ⁻¹)	1.23×10^0	8.61×10^{-1}	1.97×10^0	4.98×10^{-1}
b^S (423 K)	(kPa ⁻¹)	0.1696	0.1888	0.3913	0.2412
b^S (473 K)	(kPa ⁻¹)	0.0234	0.0248	0.0519	0.0291
b^S (523 K)	(kPa ⁻¹)	0.0047	0.0048	0.0101	0.0053
$-\Delta H^S$	(kJ/mol)	65.91	67.54	67.19	70.33
q_m^Z	(g/100 g _{ads})	—	—	1.68	2.48
b_0^Z	(kPa ⁻¹)	—	—	2.95×10^{-1}	1.72×10^0
b^Z (423 K)	(kPa ⁻¹)	—	—	8.7198	9.2124
b^Z (473 K)	(kPa ⁻¹)	—	—	0.6819	0.8628
b^Z (523 K)	(kPa ⁻¹)	—	—	0.0868	0.1271
$-\Delta H^Z$	(kJ/mol)	—	—	84.79	78.79
Δq	(g/100 g _{ads})	0.12	0.17	0.10	0.11

I, Intersection; S, Straight channel; Z, Zig-zag channel.

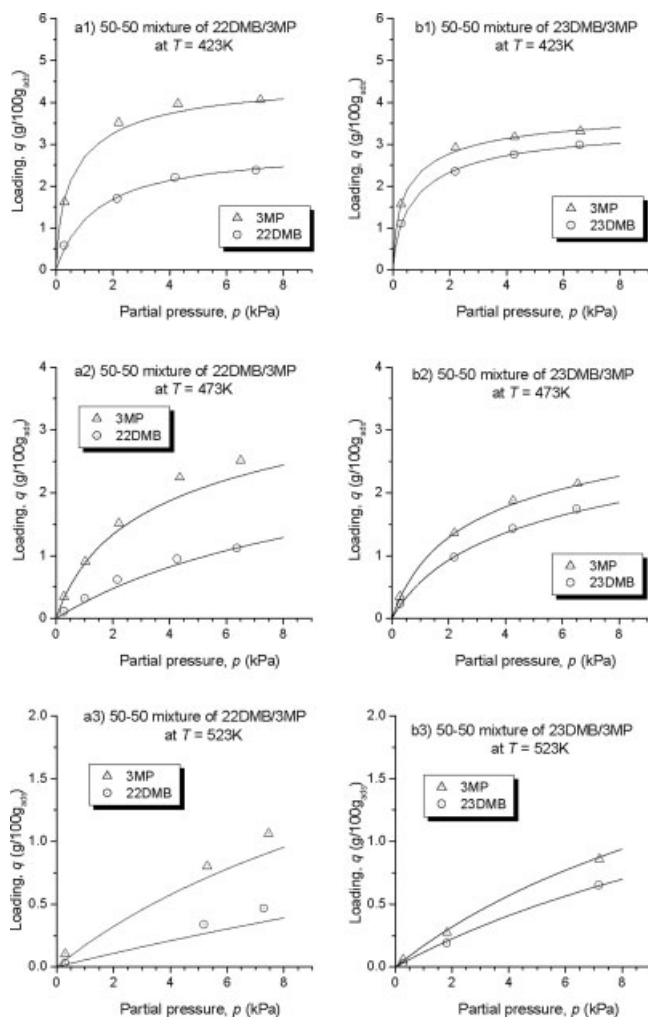


Figure 4. Binary adsorption equilibrium isotherm for an equimolar mixture of (a) 22DMB/3MP and (b) 23DMB/3MP at (1) $T = 423$ K, (2) $T = 473$ K, and (3) $T = 523$ K.

The continuous lines represent the fitting of the TSL model. The experimental conditions for the breakthrough experiments are specified in Table 4 and the isotherm model parameters in Table 3.

structure. Due to the conformation of the molecules, it was assumed that *n*HEX and 3MP can adsorb into all type of sites, instead of the bulkier dibranched molecules that cannot access to the zig-zag channels. According to this assumption, the isotherm equation describing the adsorption equilibrium of 22DMB and 23DMB should not include the term related to the zig-zag channels sites (Z).

Adsorption affinity constant, b , is assumed to vary with temperature in sites *I*, *S*, and *Z*, according to the following equation:

$$b = b_0 e^{\left(\frac{-\Delta H}{RT}\right)} \quad (3)$$

where b_0 is the frequency factor of the affinity constant, $(-\Delta H)$ is the heat of sorption, R is the universal gas constant, and T is the temperature.

The parameters of the TSL isotherm for the four pure C_6 isomers gases on zeolite BETA are determined numerically using an optimization procedure. There are 30 parameters to be determined for the four pure gas adsorption isotherms. However, it is assumed that the total saturation loading (i.e., a sum of the maximum loadings on the three sites) is constant for all isomers; consequently, this restriction eliminates some degrees of freedom from the numerical procedure.

The mean absolute deviations, $\overline{\Delta q}$, between the predicted, q , and the experimental, q_{exp} , values are calculated with

$$\overline{\Delta q} = \frac{1}{N} \sqrt{\sum_{i=1}^N (q_{\text{exp},i} - q_i)^2} \quad (4)$$

being N the total number of measurements.

Multicomponent Adsorption Isotherms. Using the parameters given by the single component adsorption equilibrium fitting, the mixture sorption data can be predicted by an extended TSL isotherm model. Accordingly, the amount adsorbed of component i , q_i , in a mixture is given by

$$q_i(p, T) = q_{m,i}^S \frac{b_i^S(T)p_i}{1 + \sum_{k=1}^n b_k^S(T)p_k} + q_{m,i}^Z \frac{b_i^Z(T)p_i}{1 + \sum_{k=1}^n b_k^Z(T)p_k} + q_{m,i}^I \frac{b_i^I(T)p_i}{1 + \sum_{k=1}^n b_k^I(T)p_k} \quad (5)$$

where n is the number of C_6 isomers in the mixture.

Numerical modeling of breakthrough experiments

The dynamic mathematical model equations used to simulate the multicomponent breakthrough curves are summarized in Table 2. This linear driving force (LDF) model has been used in previous studies^{7,10} to simulate breakthrough curves with success. The numerical solution of the model was obtained by orthogonal collocation.¹¹ The collocation points were given by the zeros of Jacobi polynomials $P_N^{(\alpha,\beta)}(x)$, with $\alpha = \beta = 0$. The resulting system was solved using a fifth order Runge-Kutta code (ODE's) in conjunction with Gauss elimination (Algebraic equations). Sixteen collocation points appeared to give satisfactory accuracy for all calculations performed.

Results and Discussion

Adsorption equilibrium

Pure Component Isotherms. The first step in the characterization of an adsorbent for a specific separation process is the measurement of the adsorption equilibrium of pure components. Pure component isotherms were determined from breakthrough experiments performed with single components diluted in helium used as the inert carrier gas. The experiments were performed at temperatures of 423, 473, and 523 K and partial pressures between 0.3 and 30 kPa. Complete information of the experimental fixed-bed runs performed, including the hydrocarbon studied, partial pressure, temperature, flowrate, mass of adsorbent used in the column, and the amount adsorbed for each run by the integration of the molar flow rate histories, is detailed elsewhere in the literature.⁷

Table 4. Experimental Conditions for Equimolar Binary, Ternary, and Quaternary Breakthrough Curves and Amount Adsorbed of Each C₆ Isomers in the Mixture; Mean Absolute Deviations Between Predicted (Extended TSL) and Measured Mixture Adsorption Equilibria on Zeolite BETA

Run	Temp. (K)	He Flow Rate, ϕ_{He} (mL/min)	C ₆ flowrate, ϕ_{C_6} ($\mu\text{mol/min}$)				Mass of Ads., W (mg)	Total Isomers Press., p_{isom} (kPa)	Amount Adsorbed, q (g/100 g _{ads})			
			22DMB	23DMB	3MP	<i>n</i> HEX			22DMB	23DMB	3MP	<i>n</i> HEX
<i>b1_1</i>	423	21.1	2.5	—	2.6	—	900	0.6	0.583	—	1.620	—
<i>b1_2</i>		5.7	5.4	—	5.5	—	900	4.4	1.702	—	3.518	—
<i>b1_3</i>		4.9	9.4	—	9.6	—	900	8.4	2.209	—	3.962	—
<i>b1_4</i>		1.7	5.8	—	5.9	—	900	14.0	2.384	—	4.057	—
<i>b1_5</i>	473	32.2	4.4	—	4.5	—	900	0.6	0.114	—	0.346	—
<i>b1_6</i>		10.2	5.4	—	5.5	—	900	2.0	0.317	—	0.904	—
<i>b1_7</i>		5.7	9.4	—	9.6	—	900	4.4	0.617	—	1.517	—
<i>b1_8</i>		4.9	6.9	—	7.1	—	900	8.4	0.946	—	2.243	—
<i>b1_9</i>		2.2	4.4	—	4.5	—	900	13.1	1.122	—	2.514	—
<i>b1_10</i>	523	10.2	1.3	—	1.3	—	900	0.6	0.033	—	0.103	—
<i>b1_11</i>		2.2	5.4	—	5.5	—	900	10.5	0.339	—	0.803	—
<i>b1_12</i>		1.3	4.6	—	4.8	—	900	14.6	0.469	—	1.062	—
<i>b2_1</i>	423	32.2	—	3.8	3.9	—	900	0.6	—	1.107	1.571	—
<i>b2_2</i>		5.7	—	5.5	5.5	—	900	4.4	—	2.352	2.916	—
<i>b2_3</i>		4.9	—	9.6	9.6	—	900	8.5	—	2.756	3.172	—
<i>b2_4</i>		2.2	—	7.0	7.1	—	900	13.2	—	2.988	3.313	—
<i>b2_5</i>	473	32.2	—	3.8	3.9	—	900	0.6	—	0.233	0.351	—
<i>b2_6</i>		5.7	—	5.5	5.5	—	900	4.4	—	0.975	1.358	—
<i>b2_7</i>		4.9	—	9.6	9.6	—	900	8.5	—	1.430	1.877	—
<i>b2_8</i>		2.2	—	7.0	7.1	—	900	13.2	—	1.743	2.148	—
<i>b2_9</i>	523	22.1	—	2.6	2.6	—	900	0.5	—	0.027	0.058	—
<i>b2_10</i>		9.7	—	7.7	7.7	—	900	3.6	—	0.191	0.273	—
<i>b2_11</i>		4.5	—	16.0	16.1	—	900	14.4	—	0.653	0.859	—
<i>t_1</i>	423	14.0	1.9	1.9	1.9	—	800	1.0	0.620	1.110	1.450	—
<i>t_2</i>		10.0	5.0	5.1	5.1	—	800	3.5	1.030	1.810	2.280	—
<i>t_3</i>		5.1	6.3	6.4	6.4	—	800	8.2	1.350	2.110	2.560	—
<i>t_4</i>		4.5	12.6	12.8	12.8	—	900	16.6	1.517	2.346	2.829	—
<i>t_5</i>	473	14.0	1.9	1.9	1.9	—	800	1.0	0.117	0.223	0.325	—
<i>t_6</i>		10.0	5.0	5.1	5.1	—	800	3.5	0.351	0.635	0.880	—
<i>t_7</i>		5.2	5.6	5.8	5.8	—	800	7.3	0.603	1.048	1.360	—
<i>t_8</i>		4.5	12.6	12.8	12.8	—	900	16.7	0.867	1.381	1.787	—
<i>t_9</i>	523	14.0	1.9	1.9	1.9	—	800	1.0	0.020	0.050	0.080	—
<i>t_10</i>		10.0	5.0	5.1	5.1	—	800	3.5	0.080	0.140	0.220	—
<i>t_11</i>		5.0	5.6	5.8	5.8	—	800	7.5	0.150	0.270	0.400	—
<i>t_12</i>		4.5	12.6	12.8	12.8	—	900	16.6	0.279	0.481	0.679	—
<i>q_1</i>	423	14.0	1.4	1.4	1.4	1.4	900	1.0	0.380	0.673	1.046	1.754
<i>q_2</i>		3.3	1.6	1.6	1.6	1.6	900	4.3	0.660	1.095	1.434	2.332
<i>q_3</i>		3.3	3.5	3.5	3.5	3.5	900	9.1	0.837	1.304	1.627	2.563
<i>q_4</i>		2.2	4.7	4.8	4.8	4.8	900	17.1	0.926	1.433	1.733	2.643
<i>q_5</i>	473	22.2	2.2	2.2	2.3	2.2	900	0.9	0.047	0.128	0.205	0.517
<i>q_6</i>		3.3	1.6	1.6	1.6	1.6	900	4.4	0.208	0.467	0.609	1.240
<i>q_7</i>		3.3	3.5	3.5	3.5	3.5	900	8.9	0.355	0.708	0.895	1.622
<i>q_8</i>		5.4	11.0	11.2	11.2	11.2	900	16.3	0.505	0.863	1.097	2.059
<i>q_9</i>	523	14.0	1.4	1.4	1.4	1.4	900	1.0	0.005	0.013	0.033	0.130
<i>q_10</i>		3.3	1.6	1.6	1.6	1.6	900	4.4	0.058	0.135	0.191	0.453
<i>q_11</i>		10.2	9.4	9.6	9.6	9.6	900	8.1	0.117	0.240	0.329	0.720
<i>q_12</i>		4.5	9.4	9.6	9.6	9.6	900	16.7	0.191	0.382	0.502	1.043

	Binary Mixture		Ternary Mixture		Quaternary Mixture	
	22DMB + 3MP	23DMB + 3MP	22DMB + 23DMB + 3MP	4-Isomers		
$\overline{\Delta}q$ (g/100 g _{ads})	0.09	0.03	0.08	0.04		

b, Binary experiments; *t*, Ternary experiments; *q*, Quaternary experiments.

Figure 3 shows the adsorption equilibrium isotherms plotted in terms of the loading in g/100 g_{ads} (wt %) as a function of the partial pressure. The equilibrium data show that *n*HEX is the component more strongly adsorbed followed by 3MP, 23DMB, and 22DMB, respectively. The amount adsorbed is considerably higher at low partial pres-

ures for *n*HEX and 3MP, but as the partial pressure increases the difference relatively to dibranched molecules decreases.

The schematic diagram at the bottom of Figure 1 allows us to discuss these results in terms of the structure of zeolite BETA. There are two types of channels with different free

aperture: the 0.66×0.67 nm straight channels; and the 0.56×0.56 -nm zig-zag channels. At low partial pressure, the lower loading of 22DMB and 23DMB in zeolite BETA can be explained by the fact that they cannot access the zig-zag channels, since these channels are too narrow for them. On the other hand, the length of 23DMB and 22DMB is lower than for *n*HEX and 3MP (see Figure 1) and this fact implies that when the partial pressure increases, the number of dibranched molecules that can be accommodated into the straight channels increases relatively to 3MP and *n*HEX. Consequently, at high partial pressures, the loading of 22DMB and 23DMB tends to approach the loading of *n*HEX and 3MP.^{6,7} This change of behavior is known as the length entropy effect.^{2,8,9,12}

As previously discussed, we assume that the existence of a slight open space (see Figure 1) at the intersection between straight and zig-zag channels can lead to a different class of active sites, when compared with the ones present along the straight and zig-zag channels. To take into account the relative importance of these possible three distinct types of active sites to the overall sorption events, it was developed the TSL model described in the theoretical section, which is suitable to fit the multicomponent isotherms to be shown later.

The fitted pure component isotherms with the TSL model are the lines in Figure 3. TSL model parameters obtained from an optimization procedure, as well as the mean absolute deviations between experimental data and predicted values are shown in Table 3. The total saturation loading (i.e., a sum of the maximum loadings on the three sites) was assumed to be constant and equal to 8 g/100 g_{ads} for all isomers. It is clear from Figure 3 that the TSL model is reasonable in predicting isotherm sorption behavior of pure C₆ isomers, for the temperatures and partial pressures studied.

Binary Adsorption Isotherms. Figures 4a1–a3 show the binary adsorption isotherms for an equimolar mixture of 22DMB/3MP and Figures 4b1–b3 for an equimolar mixture of 23DMB/3MP. The experiments were performed at 423, 473, and 523 K and partial pressure up to 7 kPa. The experimental conditions for binary experiments, as well as the amount adsorbed, are given in Table 4.

For the mixture 22DMB/3MP, Figures 4a1–a3 show that there are significant differences between the amount adsorbed of the two components being 3MP the more adsorbed one. Relatively to the equimolar mixture of 23DMB/3MP, Figures 4b1–b3 demonstrate that the difference between the amounts adsorbed is smaller than for the previous case. We also note that the extended TSL model prediction represented by the lines in Figure 4 gives a proper description of the binary adsorption data.

Ternary Adsorption Isotherms. Figures 5a–c show ternary sorption isotherms of equimolar mixtures of 22DMB/23DMB/3MP at 423, 473, and 523 K, and partial pressures up to 6 kPa. The experimental conditions for the ternary experiments are given in Table 4. This C₆ isomer mixture consists in two high RON dibranched molecules, 22DMB and 23DMB, and the 3MP low RON monobranched one. In all the ternary experiments performed, Figure 5 shows that 3MP is the more adsorbed molecule followed by 23DMB and 22DMB, respectively.

The ternary adsorption equilibrium was also fitted with the TSL model from the single-component isotherms. The TSL fitting is represented by the lines in Figure 5 and in all cases

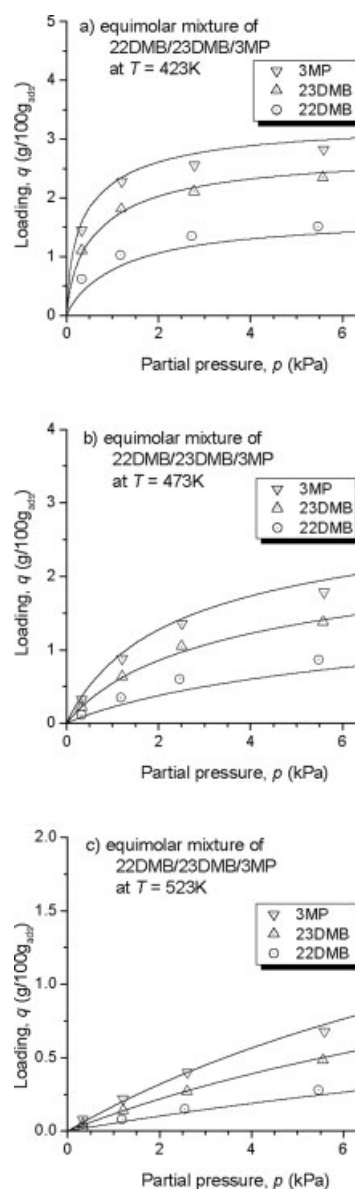


Figure 5. Ternary adsorption equilibrium isotherm for an equimolar mixture of 22DMB/23DMB/3MP on pellets of zeolite BETA.

The continuous lines represent the fitting with the TSL model. The experimental conditions for the breakthrough experiments are specified in Table 4 and the isotherm model parameters in Table 3.

it gives a good description of the ternary adsorption data for the equimolar mixture 22DMB/23DMB/3MP.

Quaternary Adsorption Isotherms. We also performed breakthrough experiments with equimolar mixtures of 22DMB/23DMB/3MP/*n*HEX at 423, 473, and 523 K, and partial pressures up to 6 kPa to determine mixture sorption isotherms. The results are shown in Figures 6a–c. In Table 4, we report the experimental conditions. In this case, we introduce in the feed to the column the linear isomer *n*HEX, which is also the lower RON molecule. We see from Figure 6 that the amount adsorbed of *n*HEX is practically the double relatively to 3MP. In terms of component loadings, the sorp-

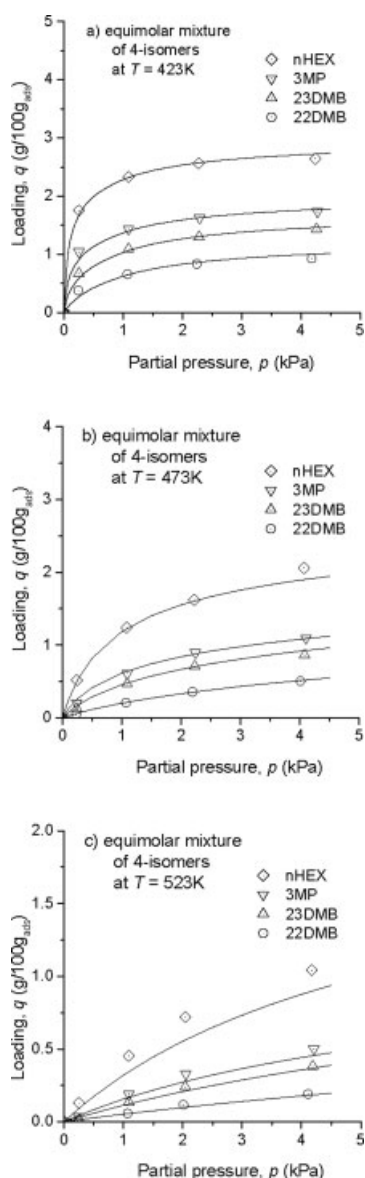


Figure 6. Quaternary adsorption equilibrium isotherm for an equimolar quaternary mixture of 22DMB/23DMB/3MP/nHEX on pellets of zeolite BETA.

The continuous lines represent the fitting with the TSL model. The experimental conditions are specified in Table 4 and the isotherm model parameters in Table 3.

tion hierarchy is $n\text{HEX} \gg 3\text{MP} > 23\text{DMB} \gg 22\text{DMB}$. This can be explained by the fact that the adsorption sites for dibranched molecules are limited to the straight channels and the intersections, while 3MP and $n\text{HEX}$ can adsorb in all type of sites of the zeolite BETA, which include zig-zag channels.

For a quantification of the ratio between the amounts adsorbed, the sorption selectivity, S , can be calculated, and for the case of an equimolar mixture, it is simply:

$$S = \frac{q_1}{q_2} \quad (6)$$

where q_1 is the adsorbed concentration of the more retained species molecule and q_2 is for the less one adsorbed component. The sorption selectivities are shown in Figures 7a1–a3 as a function of the total isomers pressure and in Figures 7b1–b3 as a function of total mixture loading for quaternary mixtures. From Figures 7a1–b3, we can conclude that at all temperatures studied the selectivity between low RON and high RON molecules decreases as the total isomers pressure and mixture loading increases. However, the values of selectivity are much higher between $n\text{HEX}/22\text{DMB}$ and $n\text{HEX}/23\text{DMB}$ relatively to the ones between 3MP/22DMB and 3MP/23DMB. An important conclusion that can be retained from these results is that to work with an acceptable selectivity for the separation of these isomers we should operate preferably at high temperature (523 K) if the total pressure

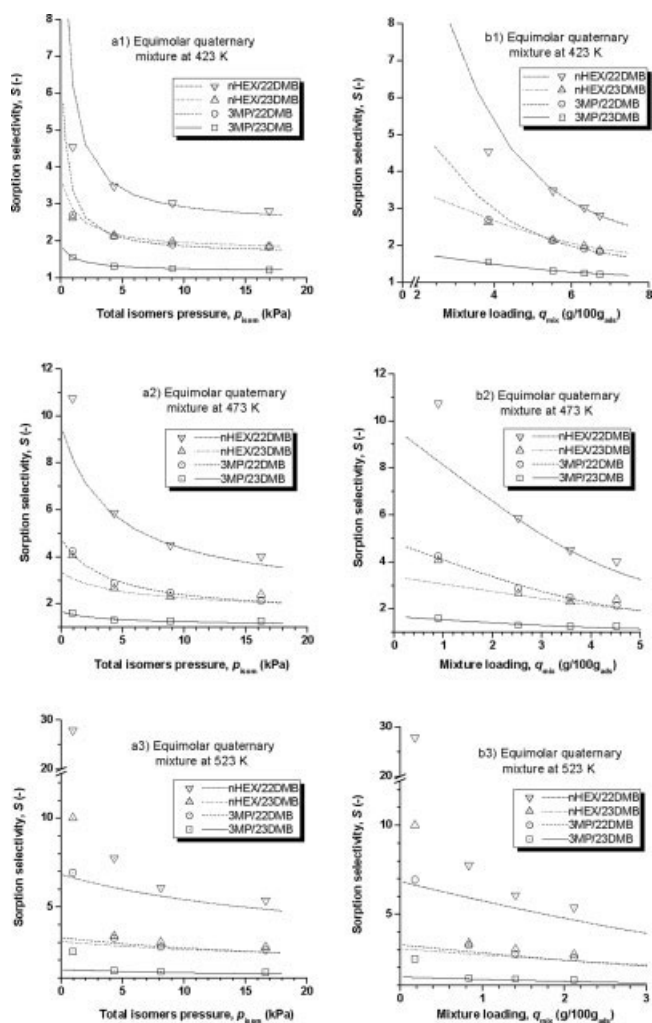


Figure 7. Effect of temperature in the sorption selectivity for an equimolar quaternary mixture of 22DMB/3MP and 23DMB/3MP as a function of (a) total isomers pressure and (b) mixture loading.

The continuous lines represent the fitting with the TSL model.

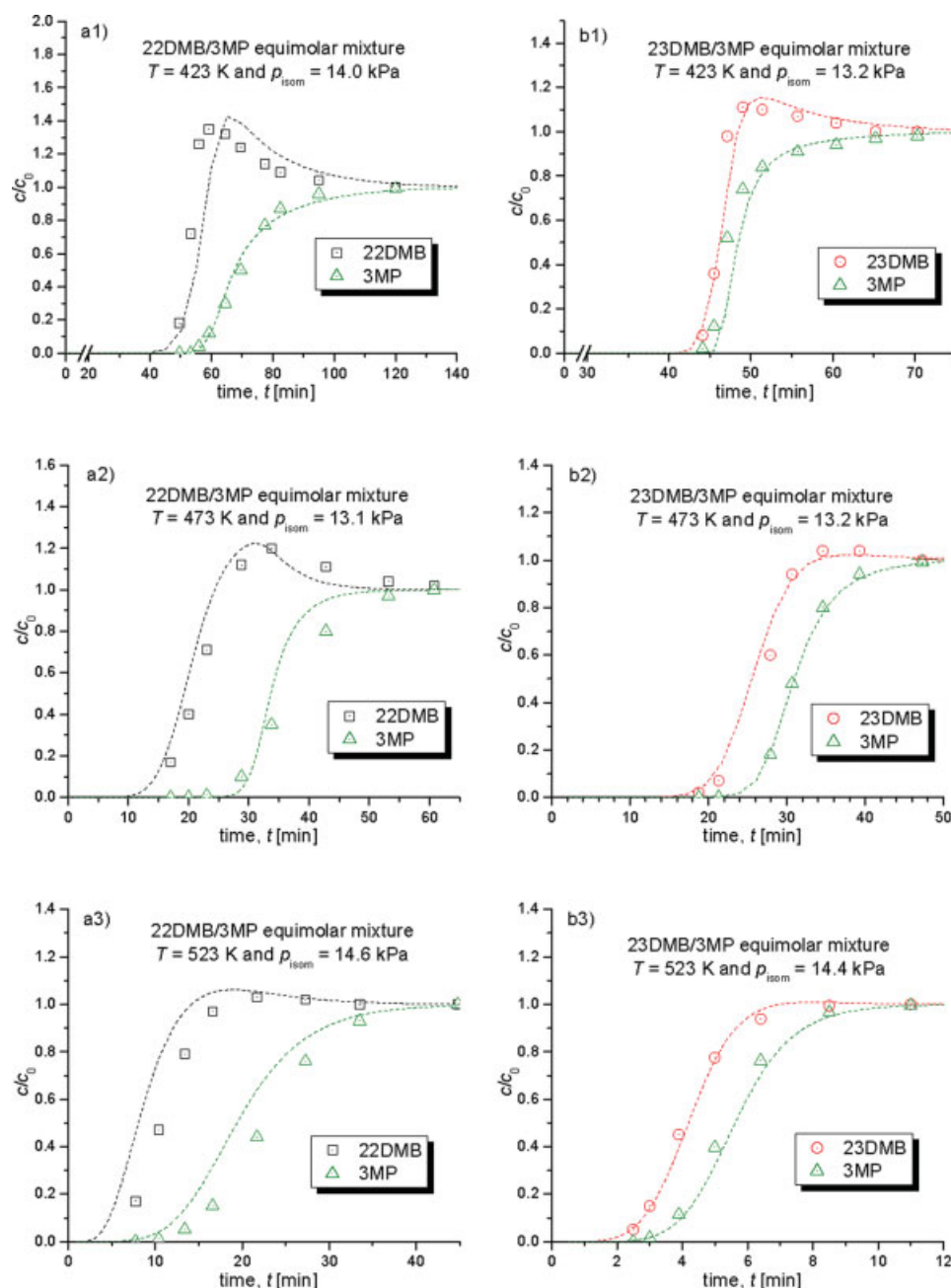


Figure 8. Effect of temperature on binary breakthrough curves for equimolar mixtures of (a) 22DMB–3MP and (b) 23DMB–3MP at (1) $T = 423$ K, (2) $T = 473$ K, and (3) $T = 523$ K at a total isomers pressure around 13 kPa.

The experimental conditions are shown in Table 4 and the model parameters in Table 5. Lines represent the dynamic mathematical model simulation and points are experimental data. [Color figure can be viewed in the online issue, which is available at www.interscience.wiley.com.]

of the paraffins in the feed range from 5 to 15 kPa. The explanation is that at these conditions the loading of the zeolite structure is not too high (lower than 1.5 g/100 g_{ads}) as can be seen in Figure 7b3. When the mixture loading increases for values higher than 4 g/100 g_{ads} the selectivity decreases significantly (see Figures 7b1,b2). We also note that the extended TSL model prediction represented by the lines in Figure 7 gives a proper description of the selectivity adsorption data.

Breakthrough curves

Influence of Temperature on Binary Breakthrough Curves of C_6 Isomers. In practice, we wish to separate the hexane isomers in a fixed bed by a proper technique. To give an overview of the typical multicomponent breakthrough curves obtained, and also to calibrate a mathematical model to be used in cyclic separation, we show the influence of temperature in a few multicomponent breakthrough curves at a fixed total isomers pressure.

Table 5. Dynamic Model Parameters for the Simulation of Multicomponent Breakthrough Curves

Run	Temp., K	Mass Transfer Coefficient, k (s^{-1})				$D_L \times 10^{-5}$, m^2/s
		22DMB	23DMB	3MP	<i>n</i> HEX	
<i>b1_2</i>	423	0.026	—	0.007	—	4.3
<i>b1_7</i>	473	0.150	—	0.038	—	5.3
<i>b1_11</i>	523	0.300	—	0.100	—	6.2
<i>b2_2</i>	423	—	0.030	0.030	—	4.3
<i>b2_6</i>	473	—	0.040	0.040	—	5.3
<i>b2_11</i>	523	—	0.100	0.100	—	6.2
<i>t_4</i>	423	0.022	0.013	0.006	—	4.4
<i>t_8</i>	473	0.100	0.060	0.015	—	5.3
<i>t_12</i>	523	0.200	0.140	0.120	—	6.2
<i>q_3</i>	423	0.014	0.006	0.003	0.021	4.4
<i>q_7</i>	473	0.055	0.014	0.008	0.055	5.3
<i>q_12</i>	523	0.100	0.060	0.060	0.100	6.3

b, Binary experiments; *t*, Ternary experiments; *q*, Quaternary experiments.

In Figure 8, the influence of temperature on breakthrough curves of binary equimolar mixtures: (a1–a3) for 22DMB/3MP and (b1–b3) for 23DMB/3MP are shown for the case where the total isomers pressure in the mixture is around 14 kPa. We plot the breakthrough curves in terms of normalized concentrations of sorbate c/c_0 , as a function of time. The experimental conditions are listed in Table 4.

We can see in Figure 8 that for both type of mixtures, the breakthrough time decreases considerably as the temperature increases. Interesting to note is the fact that at 423 K and for the mixture 22DMB/3MP, the component 3MP appears at the outlet of the column at a time of ~ 55 min compared to a time value of 40 min for 22DMB. This time difference is reasonable for a separation in a fixed bed. At 523 K, the beginning of breakthrough curve for 3MP decreases to 15 min, which compares to a time of 3 min for 22DMB. Accordingly, the breakthrough time difference between 423 and 523 K and for partial pressures around 14 kPa is practically the same. These results allow us to conclude that the selectivity observed between these isomers can lead to the development of a separation process by adsorption. We note again that for this system, as the partial pressure increases the mixture loading increases and the selectivity decreases. However, the range of partial pressures to achieve a relevant separation degree is higher at high temperatures.

For the mixture 23DMB/3MP, the separation degree is much smaller as can be seen in Figures 8b1–b3.

The prediction of breakthrough curves with the LDF-based mathematical model (see Table 2), coupled with the extended TSL isotherm model, can be seen by the lines in Figure 8. The model parameters are shown in Table 5, where the values of k can be considered as lumped parameters. It can be concluded from Figure 8 that this simple model does a surprisingly very good job, and we believe that this is due to the proper description of TSL model to account for the effects of heterogeneity of sites in the adsorbent, and consequently be able to predict with good accuracy the single and multicomponent isotherms.

Figure 8 also shows some dispersion in the shape of breakthrough curves and this is due to a combined effect of isotherm type, mass transfer resistance, and axial dispersion. Generally, type I isotherms give rise to steep breakthrough

curves; however, this effect is not so pronounced here since breakthrough curves are performed at low partial pressure.

Influence of Temperature on Ternary Breakthrough Curves of C_6 Isomers. Figure 9 shows the influence of temperature in breakthrough curves for a ternary equimolar mixture of 22DMB/23DMB/3MP at a total isomers pressure around 17 kPa.

In this case, the simultaneous presence of the three isomers reduces the difference in breakthrough time especially between 22DMB and 3MP. For instance, the breakthrough time for 3MP at 523 K is around 4 min compared to 1 min for 22DMB. However, these values are still acceptable for a separation. A direct comparison of these experiments with the ones shown in Figure 8 is not possible since the level of occupancy of the zeolite is not the same. Another interesting feature for this system is the high overshoot seen at 423 K, which practically doubles the initial concentration of 22DMB at the inlet of the column. This overshoot is an evidence of the strong interactions occurring in the zeolite due to a considerable amount of mass in the zeolite, which is in the order of 7 g/100 g_{ads} (see Figure 5). This high amount adsorbed in zeolite structure does not favor the separation.

From Figure 9, we conclude once more that the mathematical model is suitable for the prediction of the breakthrough curves, including the overshoots.

Influence of Temperature on Quaternary Breakthrough Curves of C_6 Isomers. Figures 10a–c show the effect of temperature in experimental quaternary breakthrough curves for the equimolar mixtures of *n*HEX/3MP/23DMB/22DMB in zeolite BETA at mixture total isomers pressure around 9 kPa.

In this set of experiments, we can see that *n*HEX is clearly the more strongly adsorbed component, which explains the difference in the amount adsorbed of *n*HEX relatively to the other components, already observed in the quaternary adsorption equilibrium isotherms already shown in Figure 6. It should also be noticed that the presence of *n*HEX in the mixture does not affect significantly the sorption selectivity between the mono and dibranched molecules. The mixture loading for these experiments range from ~ 7 g/100 g_{ads} at 423 K to 1.5 g/100 g_{ads} at 523 K. One interesting note is that at 523 K the component 22DMB practically does not adsorb in the column, and this can be exploited in a separation.

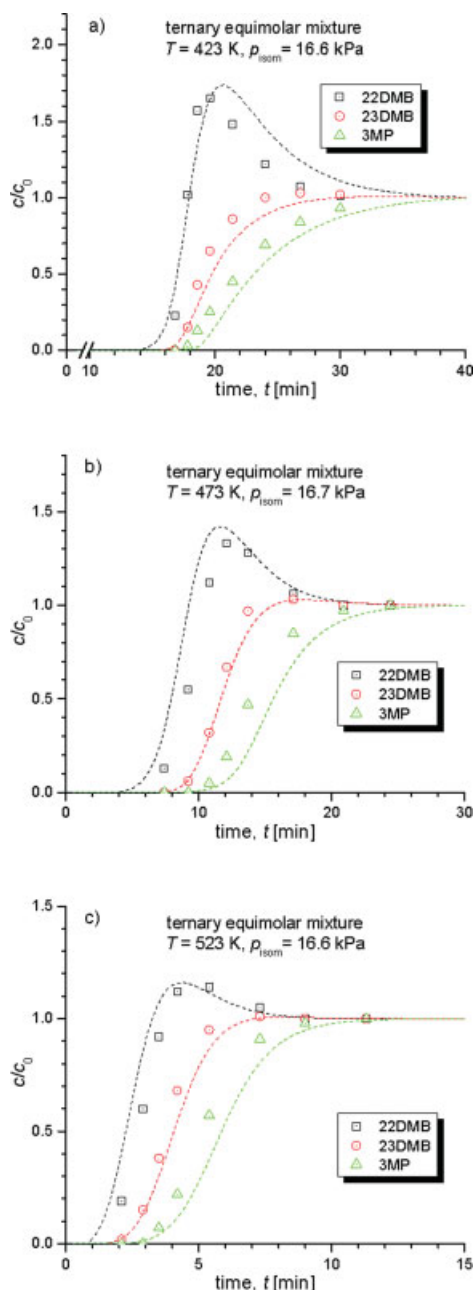


Figure 9. Effect of temperature on ternary breakthrough curves for equimolar mixtures of 22DMB-23DMB-3MP at (a) 423 K, (b) 473 K, and (c) 523 K at a total isomers pressure around 16 kPa.

The experimental conditions are shown in Table 4 and the model parameters in Table 5. Lines represent the dynamic mathematical model simulation and points are experimental data. [Color figure can be viewed in the online issue, which is available at www.interscience.wiley.com.]

The agreement between experimental data and the mathematical model is reasonably good, and this is remarkably taken into consideration that we are using a simple LDF model in a simulation of a very nonlinear multicomponent system of four adsorbable species competing with each other, in a complex zeolite structure.

Conclusions

We have presented a detailed study of sorption of hexane isomers on zeolite BETA, which includes breakthrough curves of binary, ternary, and quaternary mixtures. These experiments lead to the measurement of single and mixture sorption isotherms, and the determination of selectivities.

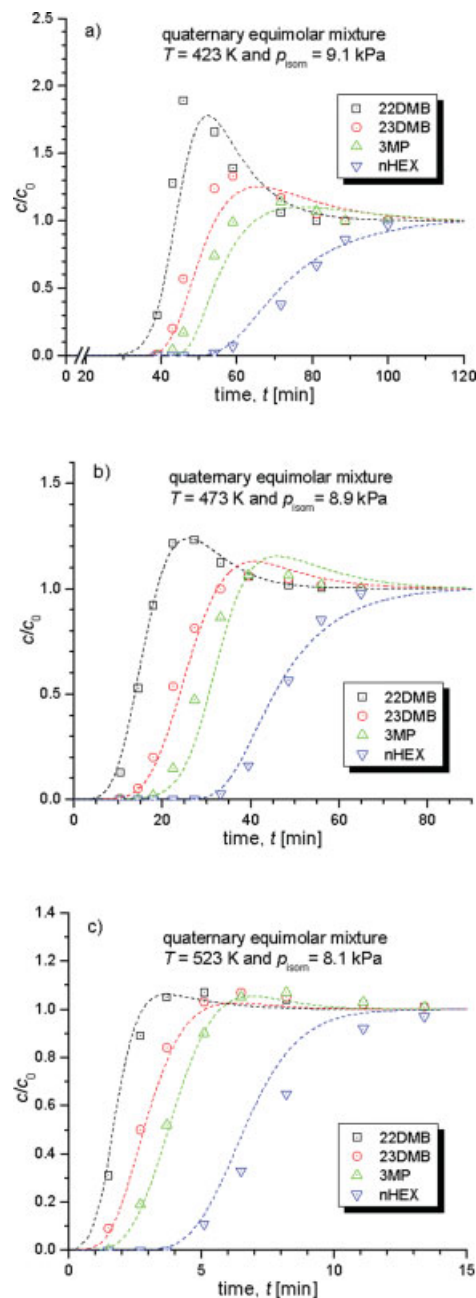


Figure 10. Effect of temperature on quaternary breakthrough curves for equimolar mixtures of 22DMB-23DMB-3MP-nHEX at (a) 423 K, (b) 473 K, and (c) 523 K at a total isomers pressure around 9 kPa.

The experimental conditions are shown in Table 4 and the model parameters in Table 5. Lines represent the dynamic mathematical model simulation and points are experimental data. [Color figure can be viewed in the online issue, which is available at www.interscience.wiley.com.]

To model sorption isotherms taking into account the complex zeolite BETA structure and consequent heterogeneity of sorption sites probably due to different types of channels, it was developed an expanded TSL isotherm model taken into account three different types of sites in the structure. The parameters of the model were obtained from the fitting of the single component isotherms of the four hexane isomers studied. Thereafter, the TSL model was extended for the prediction of mixture sorption of hexane isomers and the results compared with the experiments. A good agreement was obtained between the predictions of the TSL model and the experimental results.

Having in mind the separation of the hexane isomers in a fixed bed, a simple LDF mathematical model coupled with the TSL model isotherm was tested in its capability for the simulation of the experimental breakthrough curves. The agreement between the dynamic and experimental data is good, which opens a good perspective regarding future work.

In terms of the experimental data obtained, we conclude that the separation of hexane isomers in zeolite BETA is possible, regarding that we work at low mixture loadings, and this can be achieved at high temperatures (e.g., 523 K), if we work at lower temperatures, for instance, 423 K, the total mixture pressure should not be high.

The results arising from this study can open a window to solve the separation problem between monobranched and dibranched C₆ isomers. These data are now being used in the development of a cyclic process by an appropriate technology.

Acknowledgments

José A. C. Silva acknowledges the financial support from Fundação para a Ciência e Tecnologia under project POCI/EQU/60828/2004. Patrick S. Bárcia acknowledges a FCT grant (SFRH/BD/30994/2006).

Notation

b = affinity constant (kPa⁻¹)
 b_0 = frequency factor of the affinity constant (kPa⁻¹)
 c_0 = molar gas concentration at the inlet of the fixed bed (mol/m³)
 c_i = molar concentration of sorbate species i in the bulk gas phase (mol/m³)
 \bar{c}_i = average concentration of sorbate species i in the macropores (mol/m³)
 C = total molar gas concentration in bulk gas phase (mol/m³)
 d_k = kinetic diameter of the molecule (nm)
 D_L = axial dispersion coefficient in fixed bed (m²/s)
 D_m = molecular diffusivity (m²/s)
 ΔH = adsorption enthalpy (J/mol)
 k = mass transfer coefficient (s⁻¹)
 L = fixed bed length (m)
 n = number of hexane isomers in the mixture (—)
 N = number of experimental data points (—)
 p = partial pressure (kPa)
 p_{isom} = total isomers pressure (kPa)
 Pe = particle Peclet number (—)

q = adsorbed concentration of sorbate in the adsorbent particle (mol/kg)
 \bar{q} = average adsorbed concentration of sorbate in adsorbent particle (mol/kg)
 q_m = saturation loading capacity of sorbate in the adsorbent (mol/kg)
 q_{mix} = total loading concentration of mixture in the adsorbent (mol/kg)
 R = gas constant (J/mol/Kg)
 S = sorption selectivity (—)
 t = time (s)
 T = temperature (K)
 u = superficial velocity in packed bed (m/s)
 z = distance coordinate along fixed bed (m)

Greek letters

ρ_a = apparent density (kg/m³)
 ϵ_b = fixed bed porosity (—)
 ϵ_p = particle porosity (—)

Superscripts

I = adsorption site located at the intersection between the channels
 S = adsorption site located at the straight channels
 Z = adsorption site located at the zig-zag channels

Literature Cited

- Holcombe TC, Sager TC, Volles WK, Zarchy A. Isomerisation Process, U.S. Pat. 4,929,799, 1990.
- Schenk M, Vidal SL, Vlught TJH, Smit B, Krishna R. Separation of alkane isomers by exploiting entropy effects during adsorption on silicalite-1: a Configurational-Bias Monte Carlo simulation study. *Langmuir*. 2001;17:1558–1570.
- Jolimaitre E, Ragil K, Fayolle MT, Jallut C. Separation of mono- and dibranched hydrocarbons on silicalite. *AIChE J.* 2002;48:1927–1937.
- Davis ME, Zones SI. *Synthesis of Porous Materials: Zeolites, Clays and Nanostructures*. New York: Marcel Dekker, 1996.
- Huddersman K, Klimczyk M. Separation of branched hexane isomers using zeolite molecular sieves. *AIChE J.* 1996;42:405–408.
- Bárcia PS, Silva JAC, Rodrigues AE. Adsorption equilibrium and kinetics of branched hexane isomers in pellets of BETA zeolite. *Micropor. Mesopor. Mater.* 2005;79:145–163.
- Bárcia PS, Silva JAC, Rodrigues AE. Separation by fixed-bed adsorption of hexane isomers in zeolite BETA pellets. *Ind. Eng. Chem. Res.* 2006;45:4316–4328.
- Smit B, Krishna R. Molecular simulations in zeolitic process design. *Chem. Eng. Sci.* 2003;58:557–568.
- Krishna R, Baur R. Modelling issues in zeolite based separation processes. *Sep. Purif. Technol.* 2003;33:213–254.
- Silva FA, Silva JAC, Rodrigues AE. A general package for the simulation of cyclic adsorption processes. *Adsorption*. 1999;5:229–244.
- Villadsen JV, Michelsen ML. *Solution of Differential Equation Models by Polynomial Approximation*. Englewood Cliffs, NJ: Prentice-Hall, 1978.
- Krishna R, Vlught TJH, Smit B. Influence of isotherm inflection on diffusion in silicalite. *Chem. Eng. Sci.* 1999;54:1751–1757.
- Langer G, Roethe A, Roethe KP, Gelbin D. Heat and mass transfer in packed beds. III. Axial mass dispersion. *Int. J. Heat Mass Transf.* 1978;21:751–759.

Manuscript received Mar. 30, 2007, and final revision received May 16, 2007.